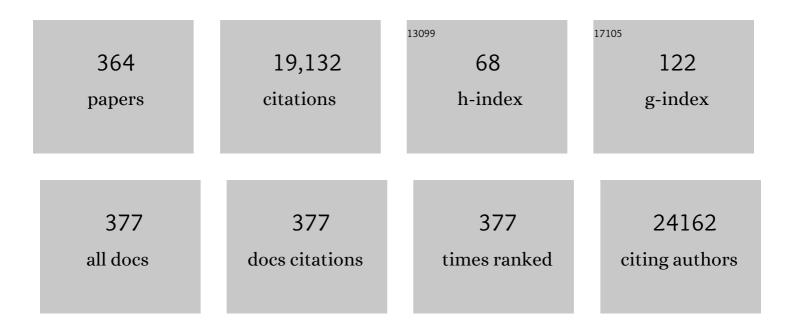
Keith J. Stevenson

List of Publications by Year in descending order

Source: https://exaly.com/author-pdf/2913291/publications.pdf Version: 2024-02-01



#	Article	IF	CITATIONS
1	Synthesis and characterization of Pt-H MoO3 catalysts for CO-tolerant PEMFCs. Catalysis Today, 2022, 388-389, 147-157.	4.4	6
2	Fluoropolymer impregnated graphite foil as a bipolar plates of vanadium flow battery. International Journal of Energy Research, 2022, 46, 10123-10132.	4.5	5
3	Composite lithium-conductive LATP+PVdF membranes: Development, optimization, and applicability for Li-TEMPO hybrid redox flow batteries. Journal of Membrane Science, 2022, 643, 120002.	8.2	8
4	Electrochemical sensors for detection of Pseudomonas aeruginosa virulence biomarkers: Principles of design and characterization. Sensors and Actuators Reports, 2022, 4, 100072.	4.4	10
5	Nickel tetrathiooxalate as a cathode material for potassium batteries. Mendeleev Communications, 2022, 32, 226-227.	1.6	1
6	Improving stability of perovskite solar cells using fullerene-polymer composite electron transport layer. Synthetic Metals, 2022, 286, 117028.	3.9	9
7	Non-Markovian diffusion of excitons in layered perovskites and transition metal dichalcogenides. Physical Chemistry Chemical Physics, 2022, 24, 13941-13950.	2.8	12
8	Cycling-Driven Electrochemical Activation of Li-Rich NMC Positive Electrodes for Li-Ion Batteries. ACS Applied Energy Materials, 2022, 5, 7758-7769.	5.1	21
9	Influence of conductive additives in a nano-impact electrochemistry study of single LiMn2O4 particles. Electrochemistry Communications, 2022, 139, 107304.	4.7	0
10	Prospect of modeling industrial scale flow batteries – From experimental data to accurate overpotential identification. Renewable and Sustainable Energy Reviews, 2022, 167, 112559.	16.4	8
11	Charge storage mechanisms of a π–d conjugated polymer for advanced alkali-ion battery anodes. Chemical Science, 2022, 13, 8161-8170.	7.4	7
12	Organic Redox Flow Batteries: Insights from Experimental and Numerical Study. ECS Meeting Abstracts, 2022, MA2022-01, 2020-2020.	0.0	0
13	Development of vanadium-based polyanion positive electrode active materials for high-voltage sodium-based batteries. Nature Communications, 2022, 13, .	12.8	35
14	Identification of Overpotentials in Vanadium Redox Flow Battery with Reference Electrodes and Determination of Apparent Electrochemical Rate Constants. ECS Meeting Abstracts, 2022, MA2022-01, 2033-2033.	0.0	0
15	(Invited) Composite Lithium-Conductive Latp+Pvdf Membranes: Development, Optimization, and Applicability for Li-Hybrid Redox Flow Batteries. ECS Meeting Abstracts, 2022, MA2022-01, 1994-1994.	0.0	0
16	(Digital Presentation) Novel Organic Materials for Non-Aqueous Redox Flow Batteries: Implementation of Triarylamine and Phenazine Core Structures. ECS Meeting Abstracts, 2022, MA2022-01, 2039-2039.	0.0	0
17	Dihydrophenazineâ€Based Copolymers as Promising Cathode Materials for Dualâ€Ion Batteries. Energy Technology, 2021, 9, .	3.8	16
18	Strength of attraction: pyrene-based hole-transport materials with effective π–Ĩ€ stacking for dopant-free perovskite solar cells. Sustainable Energy and Fuels, 2021, 5, 283-288.	4.9	6

#	Article	IF	CITATIONS
19	Solution-based chemical pre-alkaliation of metal-ion battery cathode materials for increased capacity. Journal of Materials Chemistry A, 2021, 9, 11771-11777.	10.3	11
20	Understanding the interplay between the crystal structure and charge transport in alloyed lead-free perovskites. Sustainable Energy and Fuels, 2021, 5, 5454-5460.	4.9	1
21	Polydiphenylamine as a promising high-energy cathode material for dual-ion batteries. Journal of Materials Chemistry A, 2021, 9, 2864-2871.	10.3	27
22	New phenazine based anolyte material for high voltage organic redox flow batteries. Chemical Communications, 2021, 57, 2986-2989.	4.1	33
23	Highly sensitive and selective ammonia gas sensor based on FAPbCl ₃ lead halide perovskites. Journal of Materials Chemistry C, 2021, 9, 2561-2568.	5.5	24
24	Reversible Pb ²⁺ /Pb ⁰ and I ^{â^²} /I ₃ ^{â^²} Redox Chemistry Drives the Lightâ€Induced Phase Segregation in Allâ€Inorganic Mixed Halide Perovskites. Advanced Energy Materials, 2021, 11, 2002934.	19.5	56
25	<i>m</i> -Phenylenediamine as a Building Block for Polyimide Battery Cathode Materials. ACS Applied Energy Materials, 2021, 4, 4465-4472.	5.1	21
26	Influence of hydrazinium iodide on the intrinsic photostability of MAPbI3 thin films and solar cells. Journal of Materials Research, 2021, 36, 1846-1854.	2.6	1
27	Hydroxyl Defects in LiFePO ₄ Cathode Material: DFT+ <i>U</i> and an Experimental Study. Inorganic Chemistry, 2021, 60, 5497-5506.	4.0	11
28	When iodide meets bromide: Halide mixing facilitates the light-induced decomposition of perovskite absorber films. Nano Energy, 2021, 86, 106082.	16.0	12
29	Novel Polyamine-Based Cathodes for Dual-Ion Batteries. ECS Meeting Abstracts, 2021, MA2021-01, 51-51.	0.0	0
30	(Invited) Wearable Electrochemical Sensor for Detection of Multianalyte Biomarkers in Wound Healing Efficacy. ECS Meeting Abstracts, 2021, MA2021-01, 1108-1108.	0.0	0
31	Reactive modification of zinc oxide with methylammonium iodide boosts the operational stability of perovskite solar cells. Nano Energy, 2021, 83, 105774.	16.0	22
32	Raman Spectroelectrochemical Studies of Vanadyl-Ion Oxidation on Carbon Paper Electrodes for Vanadium Redox Flow Batteries. ECS Meeting Abstracts, 2021, MA2021-01, 1784-1784.	0.0	0
33	Influence of pyridine-based ligands on photostability of MAPbI3 thin films. Mendeleev Communications, 2021, 31, 319-322.	1.6	3
34	Influence of pyridine-based ligands on photostability of MAPbI3 thin films. Mendeleev Communications, 2021, 31, 319-322.	1.6	1
35	Photochemically-Induced Phase Segregation of Mixed Halide Perovskite Solar Cells. ECS Meeting Abstracts, 2021, MA2021-01, 1809-1809.	0.0	1
36	Impact of Synthetic Route on Photovoltaic Properties of Isoindigoâ€Containing Conjugated Polymers. Macromolecular Chemistry and Physics, 2021, 222, 2100136.	2.2	1

#	Article	IF	CITATIONS
37	The Progress of Additive Engineering for CH3NH3PbI3 Photo-Active Layer in the Context of Perovskite Solar Cells. Crystals, 2021, 11, 814.	2.2	17
38	In situ spectroelectrochemical Raman studies of vanadyl-ion oxidation mechanisms on carbon paper electrodes for vanadium flow batteries. Electrochimica Acta, 2021, 383, 138300.	5.2	15
39	Combination of Metal Oxide and Polytriarylamine: A Design Principle to Improve the Stability of Perovskite Solar Cells. Energies, 2021, 14, 5115.	3.1	9
40	Chemical space mapping for multicomponent gas mixtures. Journal of Electroanalytical Chemistry, 2021, 895, 115472.	3.8	3
41	Rationalizing the effect of overstoichiometric PbI2 on the stability of perovskite solar cells in the context of precursor solution formulation. Synthetic Metals, 2021, 278, 116823.	3.9	5
42	Using structure-function relationships to understand the mechanism of phenazine-mediated extracellular electron transfer in Escherichia coli. IScience, 2021, 24, 103033.	4.1	27
43	Conjugated Ladder-Type Polymer with Hexaazatriphenylene Units as a Cathode Material for Lithium, Sodium, and Potassium Batteries. ACS Applied Energy Materials, 2021, 4, 10423-10427.	5.1	11
44	New highly soluble triarylamine-based materials as promising catholytes for redox flow batteries. Journal of Materials Chemistry A, 2021, 9, 8303-8307.	10.3	16
45	Partial Substitution of Pb ²⁺ in CsPbl ₃ as an Efficient Strategy To Design Fairly Stable All-Inorganic Perovskite Formulations. ACS Applied Materials & Interfaces, 2021, 13, 5184-5194.	8.0	21
46	Facile Method for Cross-Linking Aromatic Polyamines to Engender beyond Lithium Ion Cathodes for Dual-Ion Batteries. ACS Applied Energy Materials, 2021, 4, 11827-11835.	5.1	7
47	Effect of Polymer Binders with Single-Walled Carbon Nanotubes on the Electrochemical and Physicochemical Properties of the LiFePO ₄ Cathode. ACS Applied Energy Materials, 2021, 4, 12310-12318.	5.1	7
48	Synthesis and Characterization of Lithium-Conducting Composite Polymer–Ceramic Membranes for Use in Nonaqueous Redox Flow Batteries. ACS Applied Materials & Interfaces, 2021, 13, 53746-53757.	8.0	3
49	Trapping-influenced photoluminescence intensity decay in semiconductor nanoplatelets. Journal of Physics: Conference Series, 2021, 2015, 012103.	0.4	1
50	Revisited Ti ₂ Nb ₂ O ₉ as an Anode Material for Advanced Li-Ion Batteries. ACS Applied Materials & Interfaces, 2021, 13, 56366-56374.	8.0	8
51	Electrochemical Analysis of the Mechanism of Potassiumâ€lon Insertion into Kâ€rich Prussian Blue Materials. ChemElectroChem, 2020, 7, 761-769.	3.4	13
52	TEMPOL-promoted oxygen doping of a polytriarylamine hole-transport layer for efficient and stable lead halide perovskite solar cells. Journal of Materials Chemistry C, 2020, 8, 2419-2424.	5.5	5
53	A nickel coordination polymer derived from 1,2,4,5-tetraaminobenzene for fast and stable potassium battery anodes. Chemical Communications, 2020, 56, 1541-1544.	4.1	20
54	Phenyl-C ₆₁ -butyric Acid as an Interface Passivation Layer for Highly Efficient and Stable Perovskite Solar Cells. Journal of Physical Chemistry C, 2020, 124, 1872-1877.	3.1	32

#	Article	IF	CITATIONS
55	Correlating structure and transport properties in pristine and environmentally-aged superionic conductors based on Li1.3Al0.3Ti1.7(PO4)3 ceramics. Journal of Power Sources, 2020, 448, 227367.	7.8	25
56	Exploring the Origin of the Superior Electrochemical Performance of Hydrothermally Prepared Li-Rich Lithium Iron Phosphate Li _{1+δ} Fe _{1â^ʾδ} PO ₄ . Journal of Physical Chemistry C, 2020, 124, 126-134.	3.1	12
57	Light or Heat: What Is Killing Lead Halide Perovskites under Solar Cell Operation Conditions?. Journal of Physical Chemistry Letters, 2020, 11, 333-339.	4.6	85
58	Thermal Effects and Halide Mixing of Hybrid Perovskites: MD and XPS Studies. Journal of Physical Chemistry A, 2020, 124, 135-140.	2.5	14
59	Reduction of Methylammonium Cations as a Major Electrochemical Degradation Pathway in MAPbI ₃ Perovskite Solar Cells. Journal of Physical Chemistry Letters, 2020, 11, 221-228.	4.6	33
60	Complex diffusion-based kinetics of photoluminescence in semiconductor nanoplatelets. Physical Chemistry Chemical Physics, 2020, 22, 24686-24696.	2.8	23
61	Tellurium complex polyhalides: narrow bandgap photoactive materials for electronic applications. Journal of Materials Chemistry A, 2020, 8, 21988-21992.	10.3	8
62	Phase boundary propagation kinetics predominately limit the rate capability of NASICON-type Na3+xMnxV2-x(PO4)3 (0â‰æâ‰⊉) materials. Electrochimica Acta, 2020, 354, 136761.	5.2	26
63	Efficient and Stable MAPbI ₃ -Based Perovskite Solar Cells Using Polyvinylcarbazole Passivation. Journal of Physical Chemistry Letters, 2020, 11, 6772-6778.	4.6	48
64	A Composite Membrane Based on Sulfonated Polystyrene Implanted in a Stretched PTFE Film for Vanadium Flow Batteries. ChemPlusChem, 2020, 85, 2580-2585.	2.8	6
65	Electrochemical Detection of Multianalyte Biomarkers in Wound Healing Efficacy. ACS Sensors, 2020, 5, 3547-3557.	7.8	40
66	Perylenetetracarboxylic dianhydride as organic electron transport layer for n-i-p perovskite solar cells. Synthetic Metals, 2020, 268, 116497.	3.9	8
67	Electrochemical instability of bis(trifluoromethylsulfonyl)imide based ionic liquids as solvents in high voltage electrolytes for potassium ion batteries. Mendeleev Communications, 2020, 30, 679-682.	1.6	3
68	Film Deposition Techniques Impact the Defect Density and Photostability of MAPbI ₃ Perovskite Films. Journal of Physical Chemistry C, 2020, 124, 21378-21385.	3.1	22
69	Redox-Active Aqueous Microgels for Energy Storage Applications. Journal of Physical Chemistry Letters, 2020, 11, 10561-10565.	4.6	11
70	Decoupling Contributions of Chargeâ€Transport Interlayers to Lightâ€Induced Degradation of pâ€iâ€n Perovskite Solar Cells. Solar Rrl, 2020, 4, 2000191.	5.8	18
71	Incorporation of Vanadium(V) Oxide in Hybrid Hole Transport Layer Enables Long-term Operational Stability of Perovskite Solar Cells. Journal of Physical Chemistry Letters, 2020, 11, 5563-5568.	4.6	28
72	Electrochemical properties and evolution of the phase transformation behavior in the NASICON-type Na3+xMnxV2-x(PO4)3 (0а‰竊翁‰聲) cathodes for Na-ion batteries. Journal of Power Sources, 2020, 470, 228231.	7.8	48

#	Article	IF	CITATIONS
73	Unravelling the Material Composition Effects on the Gamma Ray Stability of Lead Halide Perovskite Solar Cells: MAPbI ₃ Breaks the Records. Journal of Physical Chemistry Letters, 2020, 11, 2630-2636.	4.6	35
74	Titanium-based potassium-ion battery positive electrode with extraordinarily high redox potential. Nature Communications, 2020, 11, 1484.	12.8	86
75	Unraveling the Impact of Hole Transport Materials on Photostability of Perovskite Films and p–i–n Solar Cells. ACS Applied Materials & Interfaces, 2020, 12, 19161-19173.	8.0	35
76	Toward Standardization of Electrochemical Impedance Spectroscopy Studies of Li-Ion Conductive Ceramics. Chemistry of Materials, 2020, 32, 2232-2241.	6.7	43
77	Active learning-based framework for optimal reaction mechanism selection from microkinetic modeling: a case study of electrocatalytic oxygen reduction reaction on carbon nanotubes. Physical Chemistry Chemical Physics, 2020, 22, 4581-4591.	2.8	5
78	Metalâ€Ion Coupled Electron Transfer Kinetics in Intercalationâ€Based Transition Metal Oxides. Advanced Energy Materials, 2020, 10, 1903933.	19.5	59
79	Complex Investigation of Water Impact on Li-Ion Conductivity of Li _{1.3} Al _{0.3} Ti _{1.7} (PO ₄) ₃ —Electrochemical, Chemical, Structural, and Morphological Aspects. Chemistry of Materials, 2020, 32, 3723-3732.	6.7	24
80	Anomalously High Proton Conduction of Interfacial Water. Journal of Physical Chemistry Letters, 2020, 11, 3623-3628.	4.6	21
81	Intrinsic thermal decomposition pathways of lead halide perovskites APbX3. Solar Energy Materials and Solar Cells, 2020, 213, 110559.	6.2	45
82	Solid-electrolyte interphase nucleation and growth on carbonaceous negative electrodes for Li-ion batteries visualized with in situ atomic force microscopy. Scientific Reports, 2020, 10, 8550.	3.3	57
83	Origins of irreversible capacity loss in hard carbon negative electrodes for potassium-ion batteries. Journal of Chemical Physics, 2020, 152, 194704.	3.0	23
84	Oxygen Reduction Reaction Mechanism Study Via the Mean-Field Microkinetic Modeling and Uncertainty Quantification of Model Parameters. ECS Transactions, 2020, 97, 757-762.	0.5	1
85	Tuning the Crystal Structure of A ₂ CoPO ₄ F (A = Li, Na) Fluorideâ€Phosphates: A New Layered Polymorph of LiNaCoPO ₄ F. European Journal of Inorganic Chemistry, 2019, 2019, 4365-4372.	2.0	7
86	Effect of Concentrated Diglyme-Based Electrolytes on the Electrochemical Performance of Potassium-Ion Batteries. ACS Applied Energy Materials, 2019, 2, 6051-6059.	5.1	44
87	Molecular Engineering of the Fullereneâ€Based Electron Transport Layer Materials for Improving Ambient Stability of Perovskite Solar Cells. Solar Rrl, 2019, 3, 1900223.	5.8	20
88	A new polytriarylamine derivative for dopant-free high-efficiency perovskite solar cells. Sustainable Energy and Fuels, 2019, 3, 2627-2632.	4.9	32
89	Electrochemical monitoring of the impact of polymicrobial infections on Pseudomonas aeruginosa and growth dependent medium. Biosensors and Bioelectronics, 2019, 142, 111538.	10.1	36
90	Impact of charge transport layers on the photochemical stability of MAPbI ₃ in thin films and perovskite solar cells. Sustainable Energy and Fuels, 2019, 3, 2705-2716.	4.9	22

20

#	Article	IF	CITATIONS
91	New tetraazapentacene-based redox-active material as a promising high-capacity organic cathode for lithium and potassium batteries. Journal of Power Sources, 2019, 435, 226724.	7.8	35
92	"Hydrotriphylites― Li _{1–<i>x</i>} Fe _{1+<i>x</i>} (PO ₄) _{1–} <i>_yas Cathode Materials for Li-ion Batteries. Chemistry of Materials, 2019, 31, 5035-5046.</i>	>(O ⊌) <sub< td=""><td>>4k\$>y<!--</td--></td></sub<>	>4 k\$ >y </td
93	Comparative Intrinsic Thermal and Photochemical Stability of Sn(II) Complex Halides as Next-Generation Materials for Lead-Free Perovskite Solar Cells. Journal of Physical Chemistry C, 2019, 123, 26862-26869.	3.1	36
94	Influence of Carbon Coating on Intercalation Kinetics and Transport Properties of LiFePO ₄ . ChemElectroChem, 2019, 6, 5090-5100.	3.4	33
95	Tuning Redox Transitions via the Inductive Effect in LaNi _{1–<i>x</i>} Fe _{<i>x</i>} O _{3â^î^} Perovskites for High-Power Asymmetric and Symmetric Pseudocapacitors. ACS Applied Energy Materials, 2019, 2, 6558-6568.	5.1	23
96	β-NaVP ₂ O ₇ as a Superior Electrode Material for Na-Ion Batteries. Chemistry of Materials, 2019, 31, 7463-7469.	6.7	31
97	Comparison of perovskite and perovskite derivatives for use in anion-based pseudocapacitor applications. Journal of Materials Chemistry A, 2019, 7, 21222-21231.	10.3	21
98	High-Energy and High-Power-Density Potassium Ion Batteries Using Dihydrophenazine-Based Polymer as Active Cathode Material. Journal of Physical Chemistry Letters, 2019, 10, 5440-5445.	4.6	68
99	Metal-ion batteries meet supercapacitors: high capacity and high rate capability rechargeable batteries with organic cathodes and a Na/K alloy anode. Chemical Communications, 2019, 55, 11758-11761.	4.1	26
100	Bifunctional OER/ORR catalytic activity in the tetrahedral YBaCo ₄ O _{7.3} oxide. Journal of Materials Chemistry A, 2019, 7, 330-341.	10.3	42
101	Decoupling the roles of carbon and metal oxides on the electrocatalytic reduction of oxygen on La _{lâ^'x} Sr _x CoO _{3â^Î^} perovskite composite electrodes. Physical Chemistry Chemical Physics, 2019, 21, 3327-3338.	2.8	26
102	Theoretical and experimental evidence for irreversible lithiation of the conformationally flexible polyimide: Impact on battery performance. Journal of Electroanalytical Chemistry, 2019, 836, 143-148.	3.8	9
103	Polymeric iodobismuthates {[Bi ₃ I ₁₀]} and {[Bil ₄]} with N-heterocyclic cations: promising perovskite-like photoactive materials for electronic devices. Journal of Materials Chemistry A, 2019, 7, 5957-5966.	10.3	53
104	Nickel(II) and Copper(II) Coordination Polymers Derived from 1,2,4,5-Tetraaminobenzene for Lithium-Ion Batteries. Chemistry of Materials, 2019, 31, 5197-5205.	6.7	52
105	New Naphthaleneâ€Based Polyimide as an Environmentâ€Friendly Organic Cathode Material for Lithium Batteries. Energy Technology, 2019, 7, 1801016.	3.8	21
106	Impressive Radiation Stability of Organic Solar Cells Based on Fullerene Derivatives and Carbazole-Containing Conjugated Polymers. ACS Applied Materials & Interfaces, 2019, 11, 21741-21748.	8.0	18
107	Efficient and stable all-inorganic perovskite solar cells based on nonstoichiometric Cs _x Pbl ₂ Br _x (<i>x</i> > 1) alloys. Journal of Materials Chemistry C, 2019, 7, 5314-5323.	5.5	30

108α-VPO₄: A Novel Many Monovalent Ion Intercalation Anode Material for Metal-Ion
Batteries. ACS Applied Materials & amp; Interfaces, 2019, 11, 12431-12440.8.0

#	Article	IF	CITATIONS
109	An ultrafast charging polyphenylamine-based cathode material for high rate lithium, sodium and potassium batteries. Journal of Materials Chemistry A, 2019, 7, 11430-11437.	10.3	62
110	Enhanced Electrocatalytic Activities by Substitutional Tuning of Nickel-Based Ruddlesden–Popper Catalysts for the Oxidation of Urea and Small Alcohols. ACS Catalysis, 2019, 9, 2664-2673.	11.2	99
111	Hexaazatriphenylene-based polymer cathode for fast and stable lithium-, sodium- and potassium-ion batteries. Journal of Materials Chemistry A, 2019, 7, 22596-22603.	10.3	80
112	Electrochemical sensors for rapid diagnosis of pathogens in real time. Analyst, The, 2019, 144, 6461-6478.	3.5	102
113	Sol-gel-modified membranes for all-organic battery based on bis-(tert-butylphenyl)nitroxide. Colloid and Polymer Science, 2019, 297, 317-323.	2.1	3
114	Poly(3,4-ethylenedioxythiophene):poly(styrenesulfonic acid)–polymer composites as functional cathode binders for high power LiFePO4 batteries. Colloid and Polymer Science, 2019, 297, 475-484.	2.1	18
115	Î ³ -Ray-Induced Degradation in the Triple-Cation Perovskite Solar Cells. Journal of Physical Chemistry Letters, 2019, 10, 813-818.	4.6	38
116	Anion-Based Pseudocapacitance of the Perovskite Library La _{1–<i>x</i>} Sr <i>_x</i> BO _{3â^î^} (B = Fe, Mn, Co). ACS Applied Materials & Interfaces, 2019, 11, 5084-5094.	8.0	60
117	Real-Time Electrochemical Detection of <i>Pseudomonas aeruginosa</i> Phenazine Metabolites Using Transparent Carbon Ultramicroelectrode Arrays. ACS Sensors, 2019, 4, 170-179.	7.8	61
118	The Role of Semilabile Oxygen Atoms for Intercalation Chemistry of the Metal-Ion Battery Polyanion Cathodes. Journal of the American Chemical Society, 2018, 140, 3994-4003.	13.7	34
119	Hybrid Solar Cells: Antimony (V) Complex Halides: Leadâ€Free Perovskiteâ€Like Materials for Hybrid Solar Cells (Adv. Energy Mater. 6/2018). Advanced Energy Materials, 2018, 8, 1870026.	19.5	1
120	Preparation and morphology characterization of core-shell water-dispersible polystyrene/poly(3,4-ethylenedioxythiophene) microparticles. Colloid and Polymer Science, 2018, 296, 737-744.	2.1	3
121	Spatial determinants of quorum signaling in a <i>Pseudomonas aeruginosa</i> infection model. Proceedings of the National Academy of Sciences of the United States of America, 2018, 115, 4779-4784.	7.1	118
122	On the Origin of Extended Resolution in Kelvin Probe Force Microscopy with a Worn Tip Apex. Microscopy and Microanalysis, 2018, 24, 126-131.	0.4	2
123	Towards understanding the origin of the hysteresis effects and threshold voltage shift in organic field-effect transistors based on the electrochemically grown AlOx dielectric. Thin Solid Films, 2018, 649, 7-11.	1.8	5
124	Teaching through Research: Alignment of Core Chemistry Competencies and Skills within a Multidisciplinary Research Framework. Journal of Chemical Education, 2018, 95, 248-258.	2.3	20
125	Improving salt-to-solvent ratio to enable high-voltage electrolyte stability for advanced Li-ion batteries. Electrochimica Acta, 2018, 263, 127-133.	5.2	19
126	Role of the Carbon Support on the Oxygen Reduction and Evolution Activities in LaNiO ₃ Composite Electrodes in Alkaline Solution. ACS Applied Energy Materials, 2018, 1, 1549-1558.	5.1	40

#	Article	IF	CITATIONS
127	Advanced porous polybenzimidazole membranes for vanadium redox batteries synthesized via a supercritical phase-inversion method. Journal of Supercritical Fluids, 2018, 137, 111-117.	3.2	37
128	Antimony (V) Complex Halides: Leadâ€Free Perovskiteâ€Like Materials for Hybrid Solar Cells. Advanced Energy Materials, 2018, 8, 1701140.	19.5	72
129	Cobalt and Vanadium Trimetaphosphate Polyanions: Synthesis, Characterization, and Electrochemical Evaluation for Non-aqueous Redox-Flow Battery Applications. Journal of the American Chemical Society, 2018, 140, 538-541.	13.7	59
130	Pretreatment of Celgard Matrices with Peroxycarbonic Acid for Subsequent Deposition of a Polydopamine Layer. Colloid Journal, 2018, 80, 761-770.	1.3	5
131	Hydrazinium-assisted stabilisation of methylammonium tin iodide for lead-free perovskite solar cells. Journal of Materials Chemistry A, 2018, 6, 21389-21395.	10.3	59
132	Theoretical study of the structure and specific capacity of an organic cathode based on poly(2,5-diaza-1,4-benzoquinone) in a lithiated state. Mendeleev Communications, 2018, 28, 239-241.	1.6	3
133	Influence of halide mixing on thermal and photochemical stability of hybrid perovskites: XPS studies. Mendeleev Communications, 2018, 28, 381-383.	1.6	10
134	Enhancing Na ⁺ Extraction Limit through High Voltage Activation of the NASICON-Type Na ₄ MnV(PO ₄) ₃ Cathode. ACS Applied Energy Materials, 2018, 1, 5842-5846.	5.1	87
135	Reversible facile Rb ⁺ and K ⁺ ions de/insertion in a KTiOPO ₄ -type RbVPO ₄ F cathode material. Journal of Materials Chemistry A, 2018, 6, 14420-14430.	10.3	34
136	A Novel Family of Polyiodoâ€Bromoantimonate(III) Complexes: Cationâ€Driven Selfâ€Assembly of Photoconductive Metalâ€Polyhalide Frameworks. Chemistry - A European Journal, 2018, 24, 14707-14711.	3.3	60
137	Understanding migration barriers for monovalent ion insertion in transition metal oxide and phosphate based cathode materials: A DFT study. Computational Materials Science, 2018, 154, 449-458.	3.0	52
138	Exceptional electrocatalytic oxygen evolution via tunable charge transfer interactions in La0.5Sr1.5Ni1â^'xFexO4±l´Ruddlesden-Popper oxides. Nature Communications, 2018, 9, 3150.	12.8	161
139	Probing the Intrinsic Thermal and Photochemical Stability of Hybrid and Inorganic Lead Halide Perovskites. Journal of Physical Chemistry Letters, 2017, 8, 1211-1218.	4.6	216
140	Structural origins of capacity fading in lithium-polyimide batteries. Journal of Materials Chemistry A, 2017, 5, 6532-6537.	10.3	29
141	Reversible and Irreversible Electric Field Induced Morphological and Interfacial Transformations of Hybrid Lead Iodide Perovskites. ACS Applied Materials & Interfaces, 2017, 9, 33478-33483.	8.0	27
142	Electrically conducting polymeric microspheres comprised of sulfonated polystyrene cores coated with poly(3,4-ethylenedioxythiophene). Colloid and Polymer Science, 2017, 295, 1049-1058.	2.1	6
143	Lithium Ion Coupled Electron-Transfer Rates in Superconcentrated Electrolytes: Exploring the Bottlenecks for Fast Charge-Transfer Rates with LiMn ₂ O ₄ Cathode Materials. Langmuir, 2017, 33, 9378-9389.	3.5	29
144	Effect of Electronâ€Transport Material on Lightâ€Induced Degradation of Inverted Planar Junction Perovskite Solar Cells. Advanced Energy Materials, 2017, 7, 1700476.	19.5	103

#	Article	IF	CITATIONS
145	Transparent Carbon Ultramicroelectrode Arrays for the Electrochemical Detection of a Bacterial Warfare Toxin, Pyocyanin. Analytical Chemistry, 2017, 89, 6285-6289.	6.5	56
146	Revealing the Chemistry and Morphology of Buried Donor/Acceptor Interfaces in Organic Photovoltaics. Journal of Physical Chemistry Letters, 2017, 8, 2764-2773.	4.6	15
147	Electrodeposition of Amorphous Molybdenum Chalcogenides from Ionic Liquids and Their Activity for the Hydrogen Evolution Reaction. Langmuir, 2017, 33, 9354-9360.	3.5	41
148	Unprecedented thermal condensation of tetracyanocyclopropanes to triazaphenalenes: a facile route for the design of novel materials for electronic applications. Chemical Communications, 2017, 53, 4830-4833.	4.1	1
149	Synthesis and charge storage properties of templated LaMnO ₃ –SiO ₂ composite materials. Dalton Transactions, 2017, 46, 977-984.	3.3	17
150	Highly Efficient All-Inorganic Planar Heterojunction Perovskite Solar Cells Produced by Thermal Coevaporation of CsI and PbI ₂ . Journal of Physical Chemistry Letters, 2017, 8, 67-72.	4.6	269
151	Gold Nanoparticle Modified Transparent Carbon Ultramicroelectrode Arrays for the Selective and Sensitive Electroanalytical Detection of Nitric Oxide. Analytical Chemistry, 2017, 89, 1267-1274.	6.5	42
152	Liquid-processed transition metal dichalcogenide films for field-effect transistors. Journal of Materials Science: Materials in Electronics, 2017, 28, 18106-18112.	2.2	1
153	Preface to the Fundamental Interfacial Science for Energy Applications Special Issue. Langmuir, 2017, 33, 9245-9245.	3.5	1
154	A materials driven approach for understanding single entity nano impact electrochemistry. Current Opinion in Electrochemistry, 2017, 6, 38-45.	4.8	91
155	Membranes based on carboxyl-containing polyacrylonitrile for applications in vanadium redox-flow batteries. Mendeleev Communications, 2017, 27, 390-391.	1.6	6
156	Polyacrylonitrile-Based Membranes for Aqueous Redox-Flow Batteries. ECS Transactions, 2017, 77, 163-171.	0.5	1
157	Spatially-resolved nanoscale measurements of grain boundary enhanced photocurrent in inorganic CsPbBr3 perovskite films. Solar Energy Materials and Solar Cells, 2017, 171, 205-212.	6.2	38
158	Influence of aminosilane precursor concentration on physicochemical properties of composite Nafion membranes for vanadium redox flow battery applications. Journal of Power Sources, 2017, 340, 32-39.	7.8	33
159	Nanostructured LaNiO ₃ Perovskite Electrocatalyst for Enhanced Urea Oxidation. ACS Catalysis, 2016, 6, 5044-5051.	11.2	217
160	Monitoring Volumetric Changes in Silicon Thin-Film Anodes through In Situ Optical Diffraction Microscopy. ACS Applied Materials & Interfaces, 2016, 8, 17642-17650.	8.0	16
161	Atomically Resolved Elucidation of the Electrochemical Covalent Molecular Grafting Mechanism of Single Layer Graphene. Advanced Materials Interfaces, 2016, 3, 1600196.	3.7	11
162	Electrocatalytic amplification of DNA-modified nanoparticle collisions via enzymatic digestion. Chemical Science, 2016, 7, 6450-6457.	7.4	32

#	Article	IF	CITATIONS
163	Mechanistic aspects of hydrazine-induced Pt colloid instability and monitoring aggregation kinetics with nanoparticle impact electroanalysis. Faraday Discussions, 2016, 193, 293-312.	3.2	9
164	Electrochemistry of single nanoparticles: general discussion. Faraday Discussions, 2016, 193, 387-413.	3.2	13
165	Direct Visualization of the Solid Electrolyte Interphase and Its Effects on Silicon Electrochemical Performance. Advanced Materials Interfaces, 2016, 3, 1600438.	3.7	59
166	Water electrolysis on La1â^'xSrxCoO3â^´Î´ perovskite electrocatalysts. Nature Communications, 2016, 7, 11053.	12.8	800
167	Addressing Colloidal Stability for Unambiguous Electroanalysis of Single Nanoparticle Impacts. Journal of Physical Chemistry Letters, 2016, 7, 2512-2517.	4.6	53
168	Switching between solid solution and two-phase regimes in the Li1-xFe1-yMnyPO4 cathode materials during lithium (de)insertion: combined PITT, in situ XRPD and electron diffraction tomography study. Electrochimica Acta, 2016, 191, 149-157.	5.2	48
169	Photo-assisted electrodeposition of MoSxfrom ionic liquids on organic-functionalized silicon photoelectrodes for H2generation. Journal of Materials Chemistry A, 2016, 4, 7027-7035.	10.3	16
170	H ₂ O ₂ Detection at Carbon Nanotubes and Nitrogen-Doped Carbon Nanotubes: Oxidation, Reduction, or Disproportionation?. Analytical Chemistry, 2015, 87, 5989-5996.	6.5	78
171	Electrochemical Activity of Dendrimer-Stabilized Tin Nanoparticles for Lithium Alloying Reactions. Langmuir, 2015, 31, 6570-6576.	3.5	10
172	Direct Evidence of a Chemical Conversion Mechanism of Atomic-Layer-Deposited TiO ₂ Anodes During Lithiation Using LiPF ₆ Salt. Journal of Physical Chemistry C, 2015, 119, 28285-28291.	3.1	10
173	Effects of Solute–Solvent Hydrogen Bonding on Nonaqueous Electrolyte Structure. Journal of Physical Chemistry Letters, 2015, 6, 2888-2891.	4.6	25
174	Increasing the Collision Rate of Particle Impact Electroanalysis with Magnetically Guided Pt-Decorated Iron Oxide Nanoparticles. ACS Nano, 2015, 9, 7583-7595.	14.6	47
175	Amperometric Detection of Aqueous Silver Ions by Inhibition of Glucose Oxidase Immobilized on Nitrogen-Doped Carbon Nanotube Electrodes. Analytical Chemistry, 2015, 87, 7250-7257.	6.5	19
176	Atom-scale covalent electrochemical modification of single-layer graphene on SiC substrates by diaryliodonium salts. Journal of Electroanalytical Chemistry, 2015, 753, 9-15.	3.8	13
177	Electrode/Electrolyte Interface of Composite α-Li ₃ V ₂ (PO ₄) ₃ Cathodes in a Nonaqueous Electrolyte for Lithium Ion Batteries and the Role of the Carbon Additive. Chemistry of Materials, 2015, 27, 3332-3340.	6.7	73
178	Electrocatalytic Amplification of Single Nanoparticle Collisions Using DNA-Modified Surfaces. Langmuir, 2015, 31, 11724-11733.	3.5	41
179	The Effect of Fluoroethylene Carbonate as an Additive on the Solid Electrolyte Interphase on Silicon Lithium-Ion Electrodes. Chemistry of Materials, 2015, 27, 5531-5542.	6.7	347
180	Transparent Carbon Ultramicroelectrode Arrays: Figures of Merit for Quantitative Spectroelectrochemistry for Biogenic Analysis of Reactive Oxygen Species. Analytical Chemistry, 2015, 87, 10109-10116.	6.5	14

#	Article	IF	CITATIONS
181	Electrochemical Modification of Indium Tin Oxide Using Di(4-nitrophenyl) Iodonium Tetrafluoroborate. Langmuir, 2015, 31, 695-702.	3.5	24
182	Controlled covalent modification of epitaxial single layer graphene on 6H-SiC (0001) with aryliodonium salts using electrochemical methods. Faraday Discussions, 2014, 172, 273-91.	3.2	20
183	Enhanced Electrochemical Oxidation of NADH at Carbon Nanotube Electrodes Using Methylene Green: Is Polymerization Necessary?. Journal of the Electrochemical Society, 2014, 161, H3042-H3048.	2.9	4
184	Role of Surface Oxides in the Formation of Solid–Electrolyte Interphases at Silicon Electrodes for Lithium-Ion Batteries. ACS Applied Materials & Interfaces, 2014, 6, 21510-21524.	8.0	110
185	Role of surface contaminants, functionalities, defects and electronic structure: general discussion. Faraday Discussions, 2014, 172, 365-395.	3.2	1
186	Wide electrochemical window ionic salt for use in electropositive metal electrodeposition and solid state Li-ion batteries. Journal of Materials Chemistry A, 2014, 2, 2194-2201.	10.3	23
187	Electrochemical Monitoring of Single Nanoparticle Collisions at Mercury-Modified Platinum Ultramicroelectrodes. ACS Nano, 2014, 8, 4539-4546.	14.6	61
188	Cathodic Electrodeposition of Amorphous Elemental Selenium from an Air- and Water-Stable Ionic Liquid. Langmuir, 2014, 30, 418-425.	3.5	14
189	Facile Fabrication of Carbon Ultramicro- to Nanoelectrode Arrays with Tunable Voltammetric Response. Analytical Chemistry, 2014, 86, 11528-11532.	6.5	24
190	The many faces of carbon in electrochemistry: general discussion. Faraday Discussions, 2014, 172, 117-137.	3.2	4
191	Single Nanoparticle Collisions at Microfluidic Microband Electrodes: The Effect of Electrode Material and Mass Transfer. Langmuir, 2014, 30, 13462-13469.	3.5	44
192	Carbon electrode interfaces for synthesis, sensing and electrocatalysis: general discussion. Faraday Discussions, 2014, 172, 497-520.	3.2	1
193	Carbon electrodes for energy storage: general discussion. Faraday Discussions, 2014, 172, 239-260.	3.2	11
194	Electrochemical and Raman spectroscopy identification of morphological and phase transformations in nanostructured TiO ₂ (B). Journal of Materials Chemistry A, 2014, 2, 20331-20337.	10.3	11
195	Investigating the Electrocatalytic Oxidation of Dihydronicotinamide Adenine Dinucleotide at Nitrogen-Doped Carbon Nanotube Electrodes: Implications to Electrochemically Measuring Dehydrogenase Enzyme Kinetics. ACS Catalysis, 2014, 4, 2969-2976.	11.2	7
196	Why here and why stay? Students' voices on the retention strategies of a widening participation university. Nurse Education Today, 2014, 34, 872-877.	3.3	22
197	Anion charge storage through oxygen intercalation in LaMnO3 perovskite pseudocapacitor electrodes. Nature Materials, 2014, 13, 726-732.	27.5	589
198	Tuning the Electrocatalytic Activity of Perovskites through Active Site Variation and Support Interactions. Chemistry of Materials, 2014, 26, 3368-3376.	6.7	229

#	Article	IF	CITATIONS
199	Electrochemical Oxidation of Dihydronicotinamide Adenine Dinucleotide at Nitrogen-Doped Carbon Nanotube Electrodes. Analytical Chemistry, 2013, 85, 9135-9141.	6.5	27
200	Room Temperature Electrodeposition of Molybdenum Sulfide for Catalytic and Photoluminescence Applications. ACS Nano, 2013, 7, 8199-8205.	14.6	92
201	Uniform epitaxial growth of Pt on Fe3O4 nanoparticles; synergetic enhancement to Pt activity for the oxygen reduction reaction. Journal of Materials Chemistry A, 2013, 1, 13443.	10.3	18
202	Control of Interface Order by Inverse Quasi-Epitaxial Growth of Squaraine/Fullerene Thin Film Photovoltaics. ACS Nano, 2013, 7, 9268-9275.	14.6	59
203	Electrochemical Behavior of Flavin Adenine Dinucleotide Adsorbed onto Carbon Nanotube and Nitrogen-Doped Carbon Nanotube Electrodes. Langmuir, 2013, 29, 13605-13613.	3.5	16
204	Size-Dependent Hydrogenation of <i>p-</i> Nitrophenol with Pd Nanoparticles Synthesized with Poly(amido)amine Dendrimer Templates. Journal of Physical Chemistry C, 2013, 117, 22644-22651.	3.1	166
205	<i>In situ</i> Raman spectroscopy of LiFePO ₄ : size and morphology dependence during charge and self-discharge. Nanotechnology, 2013, 24, 424009.	2.6	69
206	Ultrasensitive Electroanalytical Tool for Detecting, Sizing, and Evaluating the Catalytic Activity of Platinum Nanoparticles. Journal of the American Chemical Society, 2013, 135, 570-573.	13.7	145
207	A Systematic Investigation of <i>p</i> -Nitrophenol Reduction by Bimetallic Dendrimer Encapsulated Nanoparticles. Journal of Physical Chemistry C, 2013, 117, 7598-7604.	3.1	349
208	Highly Active, Nonprecious Metal Perovskite Electrocatalysts for Bifunctional Metal–Air Battery Electrodes. Journal of Physical Chemistry Letters, 2013, 4, 1254-1259.	4.6	294
209	Electrochemical Energy Storage. Accounts of Chemical Research, 2013, 46, 1051-1052.	15.6	13
210	Lithium Insertion in Nanostructured TiO ₂ (B) Architectures. Accounts of Chemical Research, 2013, 46, 1104-1112.	15.6	393
211	In Situ Raman Study of Phase Stability of α-Li ₃ V ₂ (PO ₄) ₃ upon Thermal and Laser Heating. Journal of Physical Chemistry C, 2013, 117, 11994-12002.	3.1	39
212	Electrochemically Driven Covalent Functionalization of Graphene from Fluorinated Aryl Iodonium Salts. Journal of Physical Chemistry C, 2013, 117, 12038-12044.	3.1	57
213	Influence of Surface Adsorption on the Interfacial Electron Transfer of Flavin Adenine Dinucleotide and Glucose Oxidase at Carbon Nanotube and Nitrogen-Doped Carbon Nanotube Electrodes. Analytical Chemistry, 2013, 85, 1571-1581.	6.5	87
214	Simple Methods for Production of Nanoscale Metal Oxide Films from Household Sources. Journal of Chemical Education, 2013, 90, 629-632.	2.3	6
215	Influence of the Redox Indicator Reaction on Single-Nanoparticle Collisions at Mercury- and Bismuth-Modified Pt Ultramicroelectrodes. Langmuir, 2013, 29, 15100-15106.	3.5	39
216	CONDUCTING-PROBE ATOMIC FORCE MICROSCOPY OF ELECTROCHEMICAL INTERFACES. World Scientific Series in Nanoscience and Nanotechnology, 2013, , 371-391.	0.1	2

#	Article	IF	CITATIONS
217	Nitrogen-doped Carbon Nanotube Electrodes for Enzyme Based Electrochemical Biosensing. ECS Meeting Abstracts, 2013, , .	0.0	0
218	Thermomycolin. , 2013, , 3245-3246.		0
219	Morphological Dependence of Lithium Insertion in Nanocrystalline TiO ₂ (B) Nanoparticles and Nanosheets. Journal of Physical Chemistry Letters, 2012, 3, 2015-2019.	4.6	87
220	Atomic Ensemble and Electronic Effects in Ag-Rich AgPd Nanoalloy Catalysts for Oxygen Reduction in Alkaline Media. Journal of the American Chemical Society, 2012, 134, 9812-9819.	13.7	264
221	Low-Temperature Synthesis of Amorphous FeP ₂ and Its Use as Anodes for Li Ion Batteries. Journal of the American Chemical Society, 2012, 134, 5532-5535.	13.7	131
222	Spectrophotometric Titration of Bimetallic Metal Cation Binding in Polyamido(amine) Dendrimer Templates. Analytical Chemistry, 2012, 84, 5154-5158.	6.5	12
223	Preparation and catalytic evaluation of ruthenium–nickel dendrimer encapsulated nanoparticles via intradendrimer redox displacement of nickel nanoparticles. Chemical Communications, 2012, 48, 6289.	4.1	13
224	Enhanced Charge-Transfer Kinetics by Anion Surface Modification of LiFePO ₄ . Chemistry of Materials, 2012, 24, 3212-3218.	6.7	62
225	Bifunctional Catalysts for Alkaline Oxygen Reduction Reaction via Promotion of Ligand and Ensemble Effects at Ag/MnO _{<i>x</i>} Nanodomains. Journal of Physical Chemistry C, 2012, 116, 11032-11039.	3.1	79
226	Examining Solid Electrolyte Interphase Formation on Crystalline Silicon Electrodes: Influence of Electrochemical Preparation and Ambient Exposure Conditions. Journal of Physical Chemistry C, 2012, 116, 19737-19747.	3.1	215
227	Influence of Hydrofluoric Acid Formation on Lithium Ion Insertion in Nanostructured V ₂ O ₅ . Journal of Physical Chemistry C, 2012, 116, 21208-21215.	3.1	19
228	The Effects of Aggregation on Electronic and Optical Properties of Oligothiophene Particles. ACS Nano, 2012, 6, 5507-5513.	14.6	34
229	New Nanotech from an Ancient Material: Chemistry Demonstrations Involving Carbon-Based Soot. Journal of Chemical Education, 2012, 89, 1280-1287.	2.3	28
230	LiFeO ₂ -Incorporated Li ₂ MoO ₃ as a Cathode Additive for Lithium-Ion Battery Safety. Chemistry of Materials, 2012, 24, 2673-2683.	6.7	84
231	Electrochemical Deposition of Germanium Sulfide from Room-Temperature Ionic Liquids and Subsequent Ag Doping in an Aqueous Solution. Langmuir, 2012, 28, 5513-5517.	3.5	48
232	Spectroelectrochemical Investigation of an Electrogenerated Graphitic Oxide Solid–Electrolyte Interphase. Analytical Chemistry, 2012, 84, 8190-8197.	6.5	11
233	High pseudocapacitance of MnO2 nanoparticles in graphitic disordered mesoporous carbon at high scan rates. Journal of Materials Chemistry, 2012, 22, 3160.	6.7	85
234	Carbon Optically Transparent Electrodes for Electrogenerated Chemiluminescence. Langmuir, 2012, 28, 1604-1610.	3.5	17

#	Article	IF	CITATIONS
235	Copper-Coated Amorphous Silicon Particles as an Anode Material for Lithium-Ion Batteries. Chemistry of Materials, 2012, 24, 1306-1315.	6.7	144
236	Reactive Ballistic Deposition of Nanostructured Model Materials for Electrochemical Energy Conversion and Storage. Accounts of Chemical Research, 2012, 45, 434-443.	15.6	36
237	Conducting Metallopolymers as Precursors to Fabricate Palladium Nanoparticle/Polymer Hybrids for Oxygen Reduction. Macromolecular Rapid Communications, 2012, 33, 610-615.	3.9	15
238	Influence of Mesoporosity on Lithium-Ion Storage Capacity and Rate Performance of Nanostructured TiO2(B). Langmuir, 2012, 28, 2897-2903.	3.5	72
239	The origin, development, and future of the lithium-ion battery. Journal of Solid State Electrochemistry, 2012, 16, 2017-2018.	2.5	17
240	Atomic resolution structural insights into PdPt nanoparticle–carbon interactions for the design of highly active and stable electrocatalysts. Electrochimica Acta, 2012, 64, 35-45.	5.2	19
241	Preparing students to work effectively in interprofessional health and social care teams. Quality in Primary Care, 2012, 20, 227-30.	0.8	3
242	Behavior of Li Guest in KNb ₅ O ₁₃ Host with One-Dimensional Tunnels and Multiple Interstitial Sites. Chemistry of Materials, 2011, 23, 3210-3216.	6.7	17
243	Singular Value Decomposition Analysis of Spectroelectrochemical Redox Chemistry in Supramolecular Dye Nanotubes. Journal of Physical Chemistry C, 2011, 115, 14978-14987.	3.1	10
244	Facile formation of Pt and PtPd nanoparticles on reactive carbon–TiO2 nanosheet substrates. Chemical Communications, 2011, 47, 12104.	4.1	8
245	CoMn2O4 Spinel Nanoparticles Grown on Graphene as Bifunctional Catalyst for Lithium-Air Batteries. Journal of the Electrochemical Society, 2011, 158, A1379.	2.9	218
246	Indirect Electrocatalytic Degradation of Cyanide at Nitrogen-Doped Carbon Nanotube Electrodes. Environmental Science & Technology, 2011, 45, 3650-3656.	10.0	35
247	Review of OriginPro 8.5. Journal of the American Chemical Society, 2011, 133, 5621-5621.	13.7	32
248	Silicon Nanowire Fabric as a Lithium Ion Battery Electrode Material. Journal of the American Chemical Society, 2011, 133, 20914-20921.	13.7	251
249	Morphology Dependence of the Lithium Storage Capability and Rate Performance of Amorphous TiO ₂ Electrodes. Journal of Physical Chemistry C, 2011, 115, 2585-2591.	3.1	82
250	Calculations of Li-Ion Diffusion in Olivine Phosphates. Chemistry of Materials, 2011, 23, 4032-4037.	6.7	249
251	Mechanistic Discussion of the Oxygen Reduction Reaction at Nitrogen-Doped Carbon Nanotubes. Journal of Physical Chemistry C, 2011, 115, 20002-20010.	3.1	197
252	Aqueous Electrogenerated Chemiluminescence of Self-Assembled Double-Walled Tubular J-Aggregates of Amphiphilic Cyanine Dyes. Journal of Physical Chemistry C, 2011, 115, 2470-2475.	3.1	28

#	Article	IF	CITATIONS
253	Amperometric Detection of <scp>l</scp> -Lactate Using Nitrogen-Doped Carbon Nanotubes Modified with Lactate Oxidase. Analytical Chemistry, 2011, 83, 8123-8129.	6.5	74
254	The experience of international nursing students studying for a PhD in the U.K: A qualitative study. BMC Nursing, 2011, 10, 11.	2.5	36
255	Silver–Polymer Composite Stars: Synthesis and Applications. Advanced Functional Materials, 2011, 21, 1673-1680.	14.9	44
256	A Validation of the Academic Behavioural Confidence Scale with Spanish Psychology Students. Psychology Learning and Teaching, 2011, 10, 11-24.	2.0	19
257	The learning experiences of international doctoral students with particular reference to nursing students: A literature review. International Journal of Nursing Studies, 2010, 47, 239-250.	5.6	43
258	Cathodic electrodeposition of mixed molybdenum–selenium oxides. Journal of Electroanalytical Chemistry, 2010, 638, 151-160.	3.8	8
259	Electrochemical synthesis and characterization of mixed molybdenum–rhenium oxides. Electrochimica Acta, 2010, 55, 6917-6925.	5.2	10
260	Highly-ordered mesoporous titania thin films prepared via surfactant assembly on conductive indium–tin-oxide/glass substrate and its optical properties. Thin Solid Films, 2010, 518, 3169-3176.	1.8	31
261	Grapheneâ€Based Optically Transparent Electrodes for Spectroelectrochemistry in the UV–Vis Region. Small, 2010, 6, 184-189.	10.0	86
262	Stable Oxygen Reduction Electrocatalysts from Presynthesized PdPt Nanoparticles on Carbon. ECS Transactions, 2010, 33, 161-170.	0.5	2
263	Communicating with first year medical students to improve Communication Skills teaching in The University of the West Indies. International Journal of Medical Education, 2010, 1, 5-9.	1.2	6
264	Synthesis of Pd@MoOx Electrocatalysts for Oxygen Reduction Reaction in Alkaline Media. ECS Transactions, 2010, 33, 1809-1815.	0.5	1
265	Highly Stable Pt/Ordered Graphitic Mesoporous Carbon Electrocatalysts for Oxygen Reduction. Journal of Physical Chemistry C, 2010, 114, 10796-10805.	3.1	90
266	Hybrid Generalized Ellipsometry and Quartz Crystal Microbalance Nanogravimetry for the Determination of Adsorption Isotherms on Biaxial Metal Oxide Films. Journal of Physical Chemistry Letters, 2010, 1, 1264-1268.	4.6	29
267	Enhanced Oxygen Activation over Supported Bimetallic Auâ~'Ni Catalysts. Journal of Physical Chemistry C, 2010, 114, 11498-11508.	3.1	61
268	Low Temperature Synthesis and Characterization of Nanocrystalline Titanium Carbide with Tunable Porous Architectures. Chemistry of Materials, 2010, 22, 319-329.	6.7	54
269	Photoinitiated Growth of Sub-7 nm Silver Nanowires within a Chemically Active Organic Nanotubular Template. Journal of the American Chemical Society, 2010, 132, 2104-2105.	13.7	83
270	Hybrid MnO ₂ –disordered mesoporous carbon nanocomposites: synthesis and characterization as electrochemical pseudocapacitor electrodes. Journal of Materials Chemistry, 2010, 20, 390-398.	6.7	78

#	Article	IF	CITATIONS
271	Peroxidase Mimetic Activity at Tailored Nanocarbon Electrodes. ECS Transactions, 2009, 16, 1-12.	O.5	9
272	UV-vis Spectroscopy and Cyclic Voltammetry Investigations of Tubular J-Aggregates of Amphiphilic Cyanine Dyes. ECS Transactions, 2009, 16, 77-84.	0.5	4
273	Effect of Nitrogen Concentration on Capacitance, Density of States, Electronic Conductivity, and Morphology of N-Doped Carbon Nanotube Electrodes. Journal of Physical Chemistry C, 2009, 113, 19082-19090.	3.1	341
274	Synthesis and Catalytic Evaluation of Dendrimer-Encapsulated Cu Nanoparticles. An Undergraduate Experiment Exploring Catalytic Nanomaterials. Journal of Chemical Education, 2009, 86, 368.	2.3	86
275	Software Review of Origin 8. Journal of the American Chemical Society, 2009, 131, 872-872.	13.7	37
276	Electrogenerated Chemiluminescence of Soliton Waves in Conjugated Polymers. Journal of the American Chemical Society, 2009, 131, 14166-14167.	13.7	19
277	Evaluation of Lithium Ion Insertion Reactivity via Electrochromic Diffraction-Based Imaging. Langmuir, 2009, 25, 2508-2518.	3.5	19
278	Highly Stable and Active Ptâ^'Cu Oxygen Reduction Electrocatalysts Based on Mesoporous Graphitic Carbon Supports. Chemistry of Materials, 2009, 21, 4515-4526.	6.7	109
279	Flow-Based Multiadsorbate Ellipsometric Porosimetry for the Characterization of Mesoporous Ptâ^'TiO ₂ and Auâ^'TiO ₂ Nanocomposites. Langmuir, 2009, 25, 4498-4509.	3.5	28
280	Chemical Vapor Deposition of Nanocarbon-Supported Platinum and Palladium Catalysts for Oxygen Reduction. ECS Transactions, 2008, 6, 43-50.	0.5	4
281	Electron transfer of peroxidase assemblies at tailored nanocarbon electrodes. Electrochimica Acta, 2008, 53, 6714-6721.	5.2	17
282	Spectroelectrochemical Investigation of Double-Walled Tubular J-Aggregates of Amphiphilic Cyanine Dyes. Journal of Physical Chemistry C, 2008, 112, 1260-1268.	3.1	44
283	Software Review of UN-SCAN-IT: Graph Digitizing Software. Journal of the American Chemical Society, 2008, 130, 7516-7516.	13.7	4
284	Preparation and Characterization of 3 nm Magnetic NiAu Nanoparticles. Journal of Physical Chemistry C, 2008, 112, 5365-5372.	3.1	37
285	Kinetic Evaluation of Highly Active Supported Gold Catalysts Prepared from Monolayer-Protected Clusters: An Experimental Michaelisâ Menten Approach for Determining the Oxygen Binding Constant during CO Oxidation Catalysis. Journal of the American Chemical Society, 2008, 130, 10103-10115.	13.7	81
286	Electrophoretic Deposition of Au Nanocrystals inside Perpendicular Mesochannels of TiO2. Chemistry of Materials, 2008, 20, 6029-6040.	6.7	35
287	Peroxidase Mimetic Activity at Tailored Nanocarbon Electrodes. ECS Meeting Abstracts, 2008, , .	0.0	0
288	Cathodic Electrodeposition of Mixed Rhenium-Molybdenum Oxides. ECS Transactions, 2007, 6, 17-26.	0.5	1

#	Article	IF	CITATIONS
289	Synergistic Assembly of Dendrimer-Templated Platinum Catalysts on Nitrogen-Doped Carbon Nanotube Electrodes for Oxygen Reduction. Langmuir, 2007, 23, 5279-5282.	3.5	141
290	Establishing Efficient Electrical Contact to the Weak Crystals of Triethylsilylethynyl Anthradithiophene. Chemistry of Materials, 2007, 19, 5210-5215.	6.7	39
291	Reference Electrodes. , 2007, , 73-110.		35
292	Air and Water Free Solid-Phase Synthesis of Thiol Stabilized Au Nanoparticles with Anchored, Recyclable Dendrimer Templates. Langmuir, 2007, 23, 11239-11245.	3.5	21
293	Direct Electrochemical and Spectroscopic Assessment of Heme Integrity in Multiphoton Photo-Cross-Linked CytochromecStructures. Analytical Chemistry, 2007, 79, 2303-2311.	6.5	10
294	Electrochemical Deposition and Characterization of Mixed-Valent Rhenium Oxide Films Prepared from a Perrhenate Solution. Langmuir, 2007, 23, 10837-10845.	3.5	26
295	Synthesis of an Octanuclear Eu(III) Cage from Eu42+:  Chloride Anion Encapsulation, Luminescence, and Reversible MeOH Adsorption via a Porous Supramolecular Architecture. Inorganic Chemistry, 2007, 46, 7050-7054.	4.0	53
296	Optical Constants of Electrodeposited Mixed Molybdenumâ^'Tungsten Oxide Films Determined by Variable-Angle Spectroscopic Ellipsometry. Journal of Physical Chemistry C, 2007, 111, 18251-18257.	3.1	55
297	Anomalous Electrochemical Dissolution and Passivation of Iron Growth Catalysts in Carbon Nanotubes. Langmuir, 2007, 23, 11311-11318.	3.5	69
298	Electrochemical SPM. , 2007, , 280-314.		2
299	Picomolar Peroxide Detection Using a Chemically Activated Redox Mediator and Square Wave Voltammetry. Analytical Chemistry, 2006, 78, 8518-8525.	6.5	67
300	Reversible guest molecule encapsulation in the 3-D framework of a heteropolynuclear luminescent Zn4Eu2 cage complex. Chemical Communications, 2006, , 3827.	4.1	46
301	Surface Modification of Indium Tin Oxide via Electrochemical Reduction of Aryldiazonium Cations. Langmuir, 2006, 22, 2884-2891.	3.5	116
302	Cathodic Electrodeposition of Mixed Molybdenum Tungsten Oxides from Peroxo-polymolybdotungstate Solutions. Langmuir, 2006, 22, 10490-10498.	3.5	60
303	Electrochemical oxidation of catecholamines and catechols at carbon nanotube electrodes. Analyst, The, 2006, 131, 262-267.	3.5	49
304	Patterned Assembly of Colloidal Particles by Confined Dewetting Lithography. Langmuir, 2006, 22, 11426-11435.	3.5	37
305	Nanoscale Conductivity Mapping of Hybrid Nanoarchitectures:Â Ultrathin Poly(o-phenylenediamine) on Mesoporous Manganese Oxide Ambigels. Langmuir, 2006, 22, 4462-4466.	3.5	32
306	Structure, composition, and chemical reactivity of carbon nanotubes by selective nitrogen doping. Carbon, 2006, 44, 1429-1437.	10.3	670

#	Article	IF	CITATIONS
307	High-Resolution Characterization of Pentacene/Polyaniline Interfaces in Thin-Film Transistors. Advanced Functional Materials, 2006, 16, 2409-2414.	14.9	89
308	Working with student expectations of tutor support in distance education: testing an expectationsâ€led quality assurance model. Open Learning, 2006, 21, 139-152.	4.0	15
309	Synthesis and photophysics of a porphyrin–fullerene dyad assembled through Watson–Crick hydrogen bonding. Chemical Communications, 2005, , 1892-1894.	4.1	114
310	Microfabrication of Three-Dimensional Bioelectronic Architectures. Journal of the American Chemical Society, 2005, 127, 10707-10711.	13.7	47
311	Influence of Nitrogen Doping on Oxygen Reduction Electrocatalysis at Carbon Nanofiber Electrodes. Journal of Physical Chemistry B, 2005, 109, 4707-4716.	2.6	814
312	Spatially Resolved Imaging of Inhomogeneous Charge Transfer Behavior in Polymorphous Molybdenum Oxide. I. Correlation of Localized Structural, Electronic, and Chemical Properties Using Conductive Probe Atomic Force Microscopy and Raman Microprobe Spectroscopy. Langmuir, 2005, 21, 3521-3528.	3.5	45
313	Spatially Resolved Imaging of Inhomogeneous Charge Transfer Behavior in Polymorphous Molybdenum Oxide. II. Correlation of Localized Coloration/Insertion Properties Using Spectroelectrochemical Microscopy. Langmuir, 2005, 21, 3529-3538.	3.5	12
314	No deterioration after 13 years in a stability study of a rabbit brain, plain, thromboplastin, RBT 1010, in rubber-stoppered ampoules. British Journal of Haematology, 2004, 125, 240-242.	2.5	2
315	Origin 7.5 OriginLab Corporation, One Roundhouse Plaza, Northampton, MA 01060. 1-800-969-7720. www.OriginLab.com. Suggested price \$699.00 (retail, single user), \$489.00 (educational, single user). Contact company for other pricing options Journal of the American Chemical Society, 2004, 126, 6834-6834.	13.7	1
316	Elucidation of the electrodeposition mechanism of molybdenum oxide from iso- and peroxo-polymolybdate solutions. Journal of Materials Research, 2004, 19, 429-438.	2.6	29
317	Direct Preparation of Carbon Nanofiber Electrodes via Pyrolysis of Iron(II) Phthalocyanine: Electrocatalytic Aspects for Oxygen Reduction. Journal of Physical Chemistry B, 2004, 108, 11375-11383.	2.6	270
318	Synthesis and Characterization of Dendrimer Templated Supported Bimetallic Ptâ^'Au Nanoparticles. Journal of the American Chemical Society, 2004, 126, 12949-12956.	13.7	288
319	Electrochemical quartz crystal microbalance study of the electrodeposition mechanism of molybdenum oxide thin films from peroxo-polymolybdate solution. Analytica Chimica Acta, 2003, 496, 39-51.	5.4	42
320	Electrochemical and surface characterization of platinum silicide electrodes and their use as stable platforms for electrogenerated chemiluminescence assays. Journal of Electroanalytical Chemistry, 2003, 554-555, 99-111.	3.8	9
321	Electrochemical Preparation of Molybdenum Trioxide Thin Films:Â Effect of Sintering on Electrochromic and Electroinsertion Properties. Langmuir, 2003, 19, 4316-4326.	3.5	123
322	Origin 7.0 OriginLab Corporation, One Roundhouse Plaza, Northampton, MA 01060. 1-800-969-7720. www.OriginLab.com. Suggested Price \$699.00 (Retail, Single User), \$529.00 (Educational, Single User). Contact Company for Other Pricing Options Journal of the American Chemical Society, 2003, 125, 3669-3669.	13.7	6
323	Spatially Resolved Measurement of Inhomogeneous Electrocoloration/Insertion in Polycrystalline Molybdenum Oxide Thin Films via Chronoabsorptometric Imaging. Journal of the American Chemical Society, 2003, 125, 8438-8439.	13.7	20
324	Electrochemical Synthesis of Molybdenum Oxide Thin Films: Deposition Mechanism and Template-Directed Assembly of Nanostructured Materials and Components. Materials Research Society Symposia Proceedings, 2003, 781, 111.	0.1	0

#	Article	IF	CITATIONS
325	CalculationCenter 1.0 Wolfram Research, Inc., 100 Trade Center Dr., Champaign, IL 61820-7237. http://www.wolfram.com. Suggested Retail Price:  \$295.00 Journal of the American Chemical Society, 2002, 124, 723-724.	13.7	2
326	Medical students are from Mars - business and psychology students are from Venus - University teachers are from Pluto?. Medical Teacher, 2002, 24, 27-31.	1.8	30
327	Microporous Supramolecular Coordination Compounds as Chemosensory Photonic Lattices. Angewandte Chemie - International Edition, 2002, 41, 154-157.	13.8	139
328	Monitoring Molecular Adsorption on High-Area Titanium Dioxide via Modulated Diffraction of Visible Light. Langmuir, 2001, 17, 3109-3112.	3.5	24
329	[17] Alcohol dehydrogenase from Thermococcus strain AN1. Methods in Enzymology, 2001, 331, 201-207.	1.0	6
330	Development and application of patterned conducting polymer thin films as chemoresponsive and electrochemically responsive optical diffraction gratings. Journal of Electroanalytical Chemistry, 2001, 500, 185-191.	3.8	36
331	Features of primary health care teams associated with successful quality improvement of diabetes care: a qualitative study. Family Practice, 2001, 18, 21-26.	1.9	86
332	Assembly of Micropatterned Colloidal Gold Thin Films via Microtransfer Molding and Electrophoretic Deposition. Advanced Materials, 2000, 12, 1930-1934.	21.0	74
333	University Students' Expectations of Teaching. Studies in Higher Education, 2000, 25, 309-323.	4.5	280
334	Imaging Size-Selective Permeation through Micropatterned Thin Films Using Scanning Electrochemical Microscopy. Analytical Chemistry, 2000, 72, 3122-3128.	6.5	32
335	Assembly of Micropatterned Colloidal Gold Thin Films via Microtransfer Molding and Electrophoretic Deposition. , 2000, 12, 1930.		1
336	Assembly of Micropatterned Colloidal Gold Thin Films via Microtransfer Molding and Electrophoretic Deposition. Advanced Materials, 2000, 12, 1930-1934.	21.0	2
337	"Perfect―Electrochemical Molecular Sieving by Thin and Ultrathin Metallopolymeric Films. Langmuir, 1999, 15, 837-843.	3.5	28
338	High Resolution Assembly of Patterned Metal Oxide Thin Films via Microtransfer Molding and Electrochemical Deposition Techniques. Electrochemical and Solid-State Letters, 1999, 2, 175.	2.2	19
339	Microvisualization of Structural Features and Ion Electroinsertion Behavior of Patterned WO[sub 3] Thin Films via Integrated Optical and Atomic Force Microscopies. Electrochemical and Solid-State Letters, 1999, 2, 497.	2.2	14
340	Electrochemical Measurement of the Free Energy of Adsorption ofn-Alkanethiolates at Ag(111). Journal of the American Chemical Society, 1998, 120, 1062-1069.	13.7	118
341	Voltammetric measurement of anion adsorption on Ag(111). Journal of Electroanalytical Chemistry, 1998, 447, 43-51.	3.8	53
342	Ozone levels in Chongqing: a potential threat to crop plants commonly grown in the region?. Environmental Pollution, 1998, 99, 299-308.	7.5	51

#	Article	IF	CITATIONS
343	Oxidative Adsorption ofn-Alkanethiolates at Mercury. Dependence of Adsorption Free Energy on Chain Length. Journal of Physical Chemistry B, 1998, 102, 1235-1240.	2.6	69
344	Voltammetric Measurement of Interfacial Acid/Base Reactions. Journal of Physical Chemistry B, 1998, 102, 2930-2934.	2.6	108
345	The determination of INR in stored whole blood. Journal of Clinical Pathology, 1998, 51, 360-363.	2.0	11
346	How do Open University Students Expect to be Taught at Tutorials?. Open Learning, 1998, 13, 42-46.	4.0	25
347	ELPO â€â€•a model that uses student feedback to develop effective open tutoring. Open Learning, 1997, 12, 54-59.	4.0	17
348	Calculation of System International Sensitivity Index: how many calibrant plasmas are required?. Journal of Clinical Pathology, 1997, 50, 40-44.	2.0	4
349	Local INR correction: justification for a simplified approach Journal of Clinical Pathology, 1997, 50, 783-789.	2.0	7
350	Electrochemical Deposition of Hydrosulfide and Ethanethiolate Adlayers on Silver(111). Voltammetric Measurement of Structural Phase Transitions During Adlayer Formation. Israel Journal of Chemistry, 1997, 37, 173-178.	2.3	4
351	Electrochemical Deposition of Polyborate Monolayers at Ag(111) Electrodes. Langmuir, 1997, 13, 6824-6828.	3.5	13
352	Electrochemical Oxidative Adsorption of Ethanethiolate on Ag(111). Journal of the American Chemical Society, 1997, 119, 6596-6606.	13.7	73
353	Purification and sequence analysis of a novel NADP(H)-dependent type III alcohol dehydrogenase from Thermococcus strain AN1. Journal of Bacteriology, 1997, 179, 4433-4437.	2.2	34
354	System ISI calibration: a universally applicable scheme is possible only when coumarin plasma calibrants are used. British Journal of Haematology, 1997, 96, 435-441.	2.5	18
355	Influence of Surface Defect Structure on the Underpotential Deposition of Pb Monolayers at Ag(111). Langmuir, 1996, 12, 494-499.	3.5	25
356	Student perceptions of the tutor's role in distance learning. Open Learning, 1996, 11, 22-30.	4.0	34
357	Electrochemistry of Organic Redox Liquids at Elevated Pressures. The Journal of Physical Chemistry, 1996, 100, 18818-18822.	2.9	19
358	The effect of freezing and freeze drying coumarinized plasma on international normalized ratios. Blood Coagulation and Fibrinolysis, 1995, 6, 177.	1.0	2
359	The role of lipids in the detection of lupus anticoagulant by the dilute Russell Viper venom test: are platelets or reagents containing hexagonal HIIphases necessary?. British Journal of Haematology, 1994, 86, 583-589.	2.5	21
360	The Reliability of Activated Partial Thromboplastin Time Methods and the Relationship to Lipid Composition and Ultrastructure. Thrombosis and Haemostasis, 1986, 55, 250-258.	3.4	54

#	Article	IF	CITATIONS
361	Lipid Class Composition and Heparin Sensitivity in the Activated Partial Thromboplastin Time. Thrombosis and Haemostasis, 1983, 50, 601-603.	3.4	3
362	Prediction Of Stability Of Thromboplastin. , 1981, 46, 1059.		0
363	The British Comparative Thromboplastin: the Relationship between Lipid Class Composition and Procoagulant Activity. British Journal of Haematology, 1980, 44, 495-501.	2.5	0
364	A study of empathy decline in students from five health disciplines during their first year of training. International Journal of Medical Education, 0, 2, 12-17.	1.2	230